Comparison of Stress-induced Martensitic Transformation Under Tension and Compression in Fe-28Mn-6Si-Cr Shape Memory Alloy

Bo Cao[1], and *Takeshi* Iwamoto[2,*]

[1]Graduate School of Engineering, Hiroshima University, 1-4-1 Kagamiyama, Higashi-Hiroshima, Hiroshima, Japan
[2]Institute of Engineering, Hiroshima University, 1-4-1 Kagamiyama, Higashi-Hiroshima, Hiroshima, Japan

Abstract. In the case of the NiTi alloy, some research works reported that the stress-strain curve differs significantly between tension and compression. It is considered that the difference in stress-induced martensitic transformation behavior may be observed under different loading modes in Fe-based shape memory alloy (Fe-SMA), which is less expensive compared with the widely-used NiTi alloy. In this study, both tensile and compressive tests of Fe-28Mn-6Si-5Cr shape memory alloy, which is one of Fe-SMA, are conducted under quasi-static and impact deformation at various strain rates. During deformation, it is attempted to evaluate the stress-induced martensitic transformation by measuring the volume resistivity as well as temperature for increasing a reliability of the alloy. Furthermore, from the results of volume resistivity at each strain rate, the strain rate sensitivity of stress-induced martensite under tensile and compressive tests is investigated. Additionally, the difference in stress-induced martensitic transformation under tension and compression is studied.

1 Introduction

In the previous study [1], the circuit based on the Kelvin double bridge with a higher precision is established to evaluate the change in the volume resistivity, which indirectly indicates the volume fraction of stress-induced martensite. Then, quasi-static and impact tensile tests using Fe-28Mn-6Si-5Cr shape memory alloy, which is a kind of Fe-based shape memory alloy (Fe-SMA) are conducted. In addition, during the tests, volume resistivity is measured. As a result, the change in the volume resistivity of the specimen increases during both quasi-static and impact deformation and the negative rate sensitivity can be observed.

In the case of other shape memory alloy such as NiTi, some research works reported that the stress-strain curve differs significantly between tension and compression [2-3]. The tension-compression asymmetry in stress-strain curve of Fe-SMA is also reported [4-5]. Therefore, it is possible to improve the shape memory effect of Fe-SMA by a programmed mechanical process including different loading modes.

Until now, few studies can be found about the deformation and shape recovery behaviour in Fe-SMA during compressive deformation at various strain rates, especially at higher strain rate. Therefore, it is necessary to evaluate the stress-induced martensitic transformation under such different loading modes as tension and compression at higher strain rate. In addition, it is important to capture temperature change which strongly affects the martensitic transformation. Ogawa and Yamada [6] also indicated that the temperature is a important factor for the strain rate sensitivity under compression.

In the present research work, both tensile and compressive tests of Fe-28Mn-6Si-5Cr shape memory alloy are conducted by two different testing apparatuses such as conventional material testing machine and impact testing machine based on the split Hopkinson pressure bar (SHPB) technique. During deformation, it is attempted that the relationship between the volume resistivity and true stress is measured as well as temperature-strain curve. From the results of volume resistivity at each strain rate, the strain rate sensitivity of stress-induced martensite under tensile and compressive tests is investigated. Additionally, the difference in stress-induced martensitic transformation under tension and compression is studied.

2 Experimental Procedure

2.1 Material and specimens

The material in this study is the same as the previous research work presented [1, 7]. The Fe-SMA used in this study contains four principal elements such as Fe, Mn, Si and Cr.

* Corresponding author: iwamoto@mec.hiroshima-u.ac.jp

Fig. 1 shows a photograph and geometry of specimen used in the quasi-static and impact compressive tests. The geometry of specimen used in the quasi-static and impact tensile tests is the same as the previous study [1, 7]. The specimens of Fe-SMA after machining is quenched into cold water after it is heated to 1223 K for 30 min by an electric furnace. As the result of this solution heat-treatment called shape memory treatment, residual stress caused by machining can be removed.

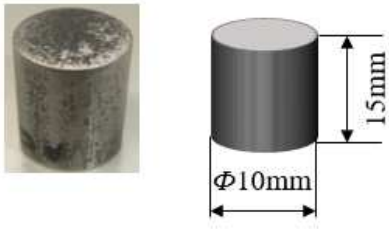

Fig. 1. A photograph and geometry of specimen used in the quasi-static and impact compressive tests.

2.2 Testing apparatuses and methods

The principle of measurement based on the Kelvin double bridge in this study is provided in the previous research work presented [1]. Compared with the previous work [1], deformation behavior during both tensile and compressive tests is mainly considered in this study. In addition, the SHPB technique is used for impact tensile and compressive tests as shown in Fig. 2. The incident wave σ_i, reflected wave σ_r and transmitted wave σ_t are detected by strain gauges. Each wire of strain gauges is connected the bridge box (Kyowa DB-120), and the output signal is amplified by the signal conditioner (Kyowa CDV-700A) as shown in Fig. 2 (b). Additionally, an impact stress-strain curve can be calculated by the theory on one-dimensional propagation of stress wave in an elastic body. The propagation of stress waves can be also seen in the Lagrange diagram of Fig. 2 (c). If the stress at two ends of the specimen is similar, it is understood that dynamic equilibrium can be achieved. More details of the calculations can be seen in Ref. [7].

In order to investigate the stress-induced martensitic transformation behaviour under different loading modes at various strain rates, quasi-static and impact tension and compression at room temperature are carried out. Additionally, Fig. 3 shows the schematic illustration on measurement in temperature during impact compressive test. Temperature is captured by an extremely-thin T-type thermocouple with 80μm in tip diameter fixed on the surface of the specimen. Moreover, it connects to a signal conditioner via an electric cold junction compensator (Omega CJ-T) and outputs a voltage signal generated by the Seebeck effect.

.

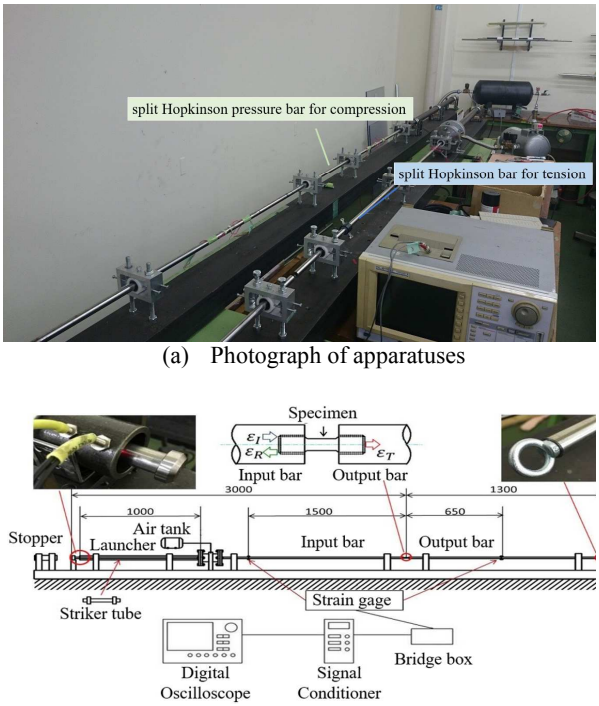

Fig. 2. (a) A photograph of the SHPB used in this study, (b) A schematic illustration of apparatus based on SHPB method for tension, (c) A schematic illustration of the SHPB for compression and the Lagrange diagram on the propagation of stress waves.

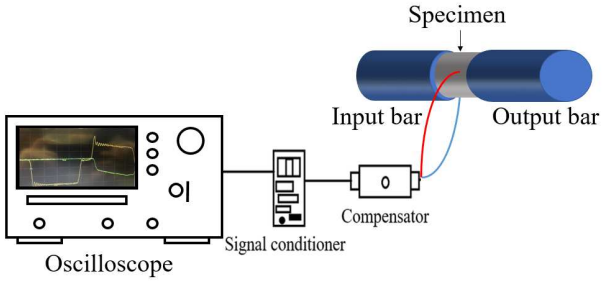

Fig. 3. A schematic illustration on measurement in temperature during impact compressive test.

3 Experimental results and discussions

3.1 Relationship between stress and strain

At first, Fig. 4 shows the time history of stress waves for impact (a) tensile and (b) compressive tests. In order to

confirm the dynamic equilibrium, each stress wave as well as the sum of σ_i and σ_r are plotted as shown in the figure. The starting time of each stress wave is shifted to 0s. As a result, it can be considered that the dynamic equilibrium is satisfied under both tension and compression. Fig. 5 shows the time history of strain rate under tensile and compressive tests calculated by the waves in Fig. 4. In order to facilitate a comparison, the strain rate of compressive test is converted to be positive. As shown in this figure, strain rate keeps almost constant during impact tensile deformation. On the other hand, compressive strain rate changes drastically. The average strain rate of tension and compression can be calculated as a representative value and they are 443 and 227 /s, respectively.

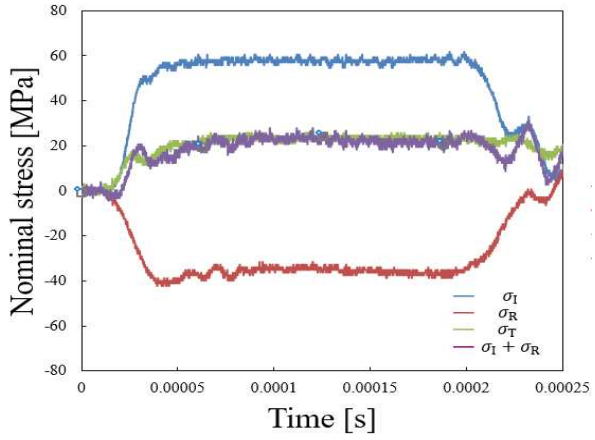

(a) Tension

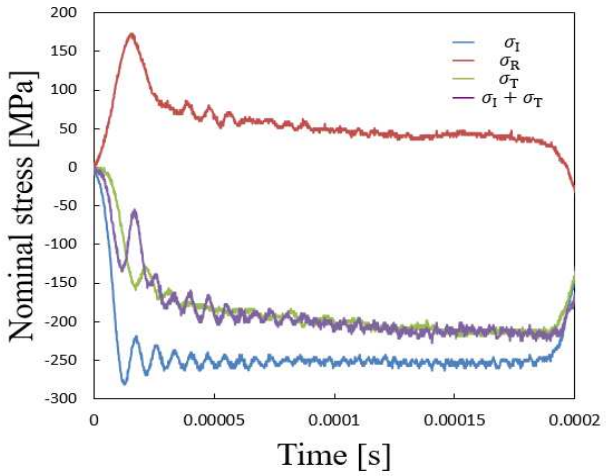

(b) Compression

Fig. 4. Time history of stress wave after each wave separated under tension and compression.

Next, Fig. 6 shows the relationship between true stress and true strain during tensile and compressive deformation at two strain rates. As shown in this figure, the stress-strain curve in Fe-SMA is similar to that in conventional metallic materials with properties of ductile materials. The non-linearity affected by the formation of stress-induced martensitic transformation as well as plastic deformation can be observed. Compared with the result of tension under quasi-static and impact deformation, the stress level of compression becomes higher. In addition, the stress level increases with increasing strain rate during both tensile and compressive deformation. That is, a positive rate sensitivity of stress in Fe-SMA, can be clearly shown under both tensile and compressive deformation.

In order to clarify the rate sensitivity of stress between tension and compression, the relationship between true stress and strain rate at the 0.025 of true strain is given in Fig. 7. As shown in this figure, positive strain rate sensitivity can be seen. In this figure, the true stress at 0.025 of true strain under quasi-static and impact compression at room temperature are 479 and 539 MPa, respectively. These values are similar the result obtained by Ogawa and Yamada [6]. Similar result of positive rate sensitivity in Fe-SMA under compressive deformation can be also seen in Ref. [6]. The linear curve represents the strain rate sensitivity exponent m =d(lnσ)/d(lnε̇). The values of slopes in tensile and compressive curve are 0.0082 and 0.0119, respectively. Of course, this comparison is insufficient with less number of experimental data.

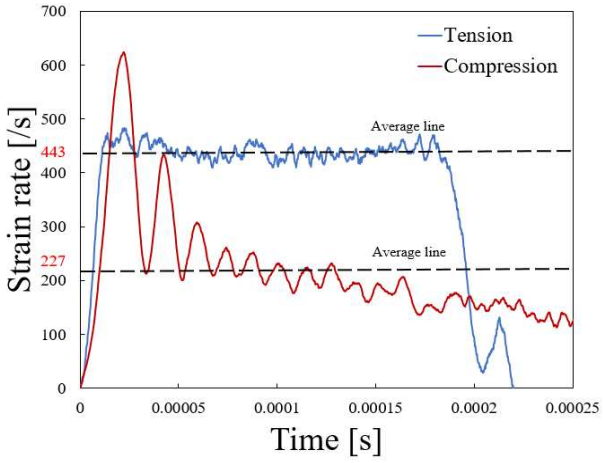

Fig. 5. Time history of strain rate in the impact tensile and compressive tests.

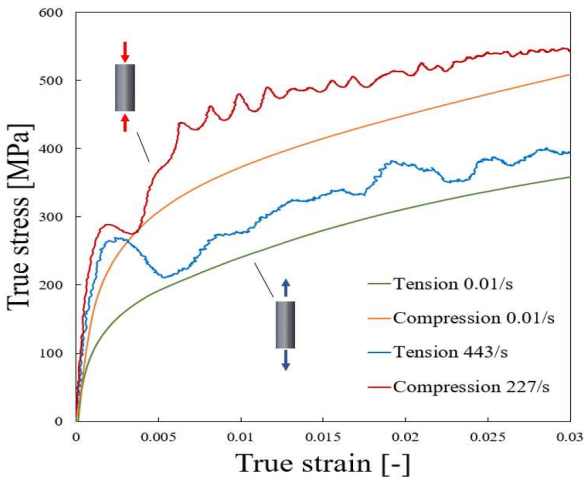

Fig. 6. Relationship between true stress and true strain at various strain rates from quasi-static to impact levels under tension and compression.

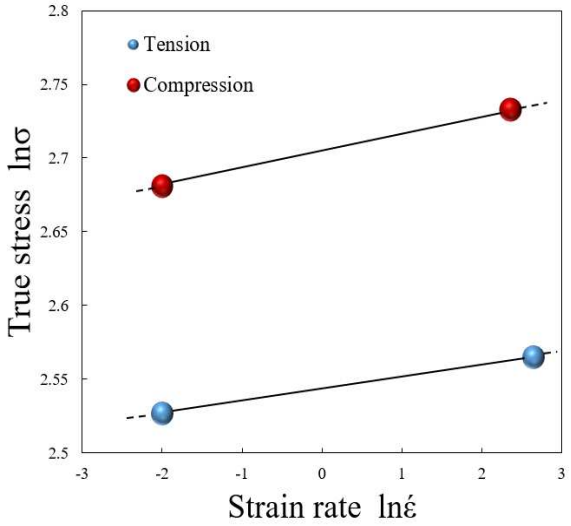

Fig. 7. True stress at 0.025 of true strain to strain rate relation obtained at tensile and compressive tests.

3.2 Relationship between temperature rise and strain

In order to obtained reliability of the measurement as well as validity of measured temperature rise at higher strain rate, the responsivity and accuracy of temperature measurement must be higher. In the past, Kobayashi et al. [8] indicated the responsivity of the infrared detector is higher than the thermocouple, which the thermocouple is the K-type with 200 μm in tip-diameter. However, Rittel et al. [9, 10] issue the different viewpoint. They found that the infrared detector and T-type thermocouple with 125 μm in tip-diameter can measure a very similar evolution of the temperature with the infrared detector. Even in the case at 8000 /s of strain rate, the thermocouple works better.

Then, Fig. 8 shows the relationship between temperature rise and true strain during tensile and compressive deformation. From this figure, it can be seen that the temperature increases with increasing strain rate. This means, the positive rate sensitivity of the temperature can be seen. The similar tendency of temperature rise under quasi-static and impact tension and compression can be obtained. As a consequence, almost concave curve can be obtained at each strain rate. When the strain rate is relatively lower, it is difficult to ignore the influence of natural convection by the air on the surface temperature of the specimen as the heat transfer. When the strain rate becomes larger, the heat transfer is insignificant and adiabatic condition can be achieved. Then, in order to check the responsivity of thermocouple used in this study, the time history of plastic strain and change in temperature under impact compression is shown in Fig. 9. In this figure, the slope of temperature rise decreases rapidly when plastic deformation ends. Therefore, high responsivity of thermocouple can be confirmed from this figure.

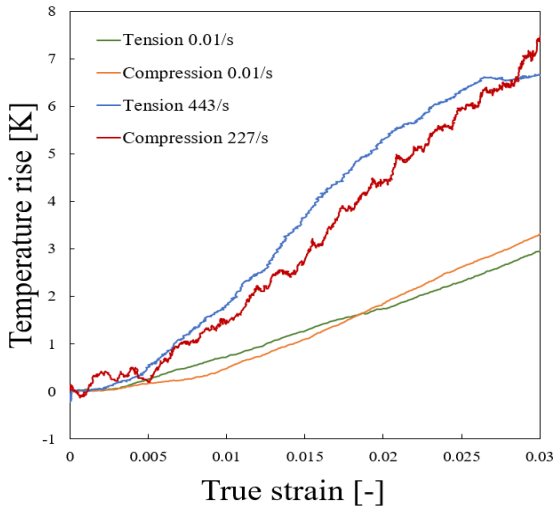

Fig. 8. Relationship between temperature rise and true strain at various strain rates.

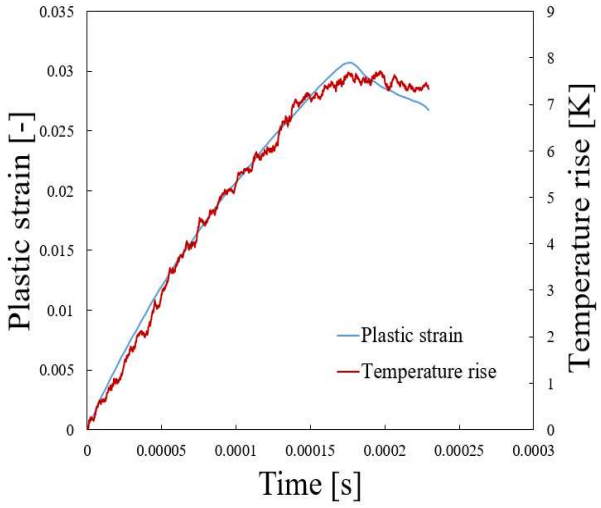

Fig. 9. Time history of plastic strain and change in temperature under compression.

3.3 Relationship between the change in volume resistivity and stress

Figure 10 shows the relationship between the change in resistance of the specimen and true strain at various strain rates. As shown in this figure, convex curves with respect to strain can be seen. In addition, it can be observed that the change in resistance becomes smaller at higher strain rate under both tensile and compressive deformation. Let us focus on the case of the quasi-static tests, a plateau-like region in the curve under both quasi-static tensile and compressive tests is observed.

Next, the relationship between the change in the volume resistivity of specimens and true stress during tensile and compressive deformation at various strain rates is presented in Fig. 11 calculated from Fig. 10. As shown in this figure, the parabolic curve with respect to the stress can be observed. The change in the volume resistivity of the specimen starts increasing as stress increases during deformation when the stress achieves a certain level. Additionally, the change in the volume

resistivity at lower strain rate under both tension and compression becomes larger than that at higher strain rate. From this figure, it is difficult to observe the change in volume resistivity under tension at strain rate of 443 /s. As a result, it is successful to capture the strain rate sensitivity. Totally, it can be considered that the sensitivity should be negative. This may be the reason of suppressing martensitic transformation by temperature rise as shown in Fig. 8. The temperature during deformation strongly affects the phase stability and the stacking fault energy in the austenite [11]. On the other hand, compared with the case of tension, the change in volume resistivity under compression becomes larger. It is plausible that it leads to the higher strain rate sensitivity of compression as shown in Fig. 7. It means that the volume fraction of stress-induced martensite in this alloy is influenced not only by temperature but also by the loading mode.

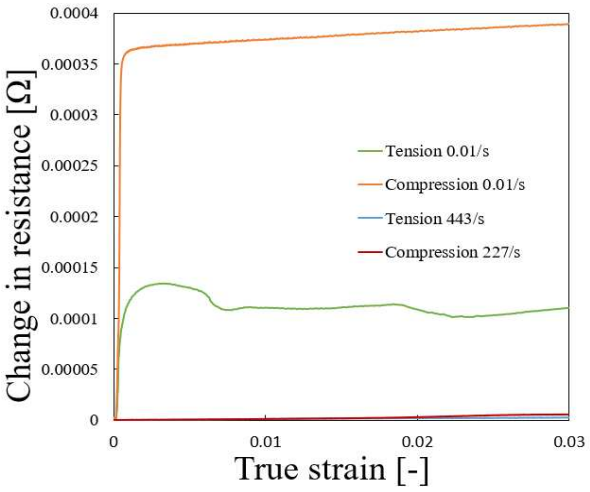

Fig. 10. Relationship between the change in resistance and true strain at various strain rates.

In addition, Yoshikawa et al. [12] investigated the martensitic transformation by 0.02% proof stress of Fe-SMA under various loading condition. As the result, the martensitic transformation behaviour cannot be distinguished under various low stress loading condition. However, quantification of stress-induced martensite has not been done. In the past, Stanford and Dunne [4] conducted the bending tests of Fe-SMA. As a result, it reported that the region subjected to compressive stress has more rumpled surface relief than the region subjected to tensile stress. It proves the the change in volume resistivity under compression becomes larger than that of tension as shown in Fig. 11.

4 Concluding remarks

In this study, both tensile and compressive tests of Fe-28Mn-6Si-5Cr alloy, which is the commercially-supplied Fe-SMA, were conducted by conventional material testing machine and impact testing machine based on the split Hopkinson tensile and pressure bar technique. By using the previously-manufactured circuit based on the Kelvin double bridge, it was attempted that the relationship between resistance and true strain under the quasi-static and impact tensile test was measured as well as temperature-strain curve. As a result, it was successful to capture the changes in volume resistivity of Fe-SMA during both tensile and compressive deformation at various strain rates. Furthermore, the temperature-strain curves were measured. Other detailed results will be discussed at the conference.

We gratefully acknowledge financial supports from THE AMADA FOUNDATION and the 26th ISIJ Research Promotion Grant, Japan.

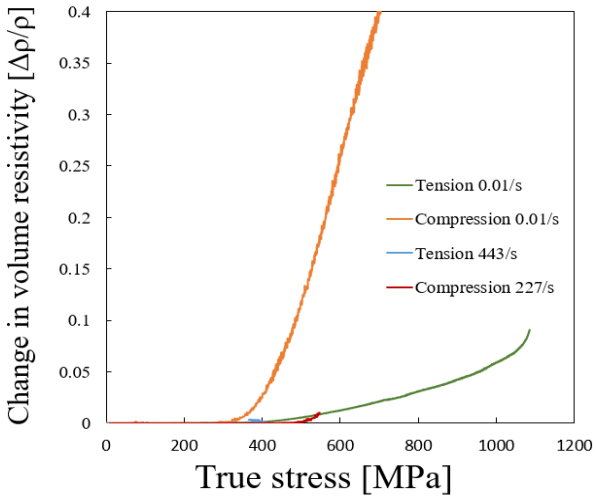

Fig. 11. Relationship between the change in volume resistivity and true stress at various strain rates.

References

1. B. Cao, T. Iwamoto, Int. J. Mech. Sci. (2018), to be published
2. C. Elibol, M. F. -X. Wagner, Mater. Sci. Eng. A, **621** (2015)
3. L. Orgéas, D. Favier, Acta. Mater, **46** (1998)
4. N. Stanford, D. Dunne, Scripta. Mater, **53** (2005)
5. J. Ma, B. Kockar, A. Evirgen, I. Karaman, Z. P. Luo, Y. I. Chumlyakov, Acta. Mater, **60** (2012)
6. K. Ogawa, A. Yamada, J. Soc. Mater. Sci, Jpn, **40** (1991) (in Japanese)
7. T. Iwamoto, K. Fujita, *Proceeding ESOMAT2015* (Matec Web Conf, 33, EDP sciences 2015)
8. H. Kobayashi, F. Okada, K. Ogawa, K. Horikawa, K. Watanabe, J. Soc. Mater. Sci, Jpn, **62** (2013) (in Japanese)
9. A. Regev, D. Rittel, Exp. Mech, **48** (2008)
10. D. Rittel, Exp, Mech, **38** (1998)
11. W. Tasaki, T. Sawaguchi, I. Nikulin, K. Sekido, K. Tsuchiya, Mater. Trans, **57** (2016)
12. T. Yoshikawa, T. Inaba, K. Ida, S. Mizutani, *Advances in shape memory materials* (Springer, 2017)